Stereovision Based Leader/Follower Tracking control for Nonholonomic Mobile Robots

Zeghlache SAMIR and Mohand Saïd DJOUADI

Laboratoire robotique & productique,
Ecole militaire polytechnique, Bp : 17 Bordj El Bahri 16111 Alger, Algérie.

zeghlache_samir@yahoo.fr, msdjouadi@gmail.com

***Abstract*- This work discusses a control strategies to solve the target tracking problem for nonholonomic mobile robots, in our experiments we have considered two robots, a leader and a follower. The follower robot tracks a target (leader) moving along an unknown trajectory. It uses only stereovision to establish its both relative position and orientation to the target, so as to maintain a specified and a given distance between the two robots. Experimental results are included and discussed to show the performances of the proposed vision-based tracking control system.**

***Keywords*— mobile robot, stereovision, vision based control, Lyapunov theory**

I. INTRODUCTION

In the recent years, efforts have been made to give autonomy to mobile robots by using different sensors to collect information from the surroundings and react to the changes of its immediate environment. Computer vision is one of the most popular perception sensors employed for autonomous robots. In many task such as surveillance and grasping, visual path tracking, visual tracking of a moving object. The application of vision based tracking control design for robotic application has been an active area of robotic research, the papers [1,2] present study of visual servoing approaches for tracking control of non-holonomic mobile robots, in [3] the authors present study of visual navigation mobile robots, this work subdivided into the visual navigation in indoor environment and the visual navigation in outdoor environment. A method and illustration of vision data extraction is also presented, in order to allow a robot to operate in an unknown and dynamic environment. In [4] the authors have presented a vision-based scheme for driving a non-holonomic mobile robot to intercept a moving target, on the lower level, the pan-tilt platform which carries the on-board camera is controlled so as to keep the target at the centre of the image plane; on the higher level, the robot operates under the assumption that the camera system achieves perfect tracking. In particular, the relative position of the ball is retrieved from the pan-tilt angles through simple geometry, and used to compute a control law driving the robot to the target. Various possible choices are discussed for the high-level robot controller. In [5] a robust visual tracking controller is proposed for tracking control of a mobile robot in image plan, this work based on the proposed error-state model, the visual tracking control problem is transformed into the stability problem. The robust control law is then proposed to guarantee that the visual tracking system satisfies the necessary stability condition based on LYAPUNOV theory. [6] Describes the position control of autonomous mobile robot using combination of kalman filter and fuzzy logic technique. Both techniques have been used to fuse information from internal and external sensors to navigate the mobile robot in unknown environment. An obstacle avoidance algorithm using stereovision technique has been implemented for obstacle detection. [7] Presents a strategy for a non-holonomic mobile robot to autonomously follow a target based on vision information from an onboard pan camera unit. Homography based techniques are used to obtain relative position and orientation information from the monocular camera images. The proposed kinematic controller, based on the Lyapunov method, achieves uniform ultimately bounded tracking. In [8] and [9] the authors have proposed the state feedback control using the fuzzy logic controller to realize a leader and follower mobile robot based on laser and infrared sensors.

The monocular vision based tracking control suffers to obtain the 3D target position. However, in our work the stereovision system has been used to solve this problem, we can at each instant have a pair of images, from two geometrical defined cameras, that allow us to have four image coordinates. The triangulation equation is used to estimate the relative 3D position (tracker-target). In this paper we aim to ensure an accurate tracking in case of a leader/follower mobile robot scheme, by experimenting different stereovision based control strategies. First we will describe the kinematical model of a mobile robot (Section II), and the camera model (section III), section IV present the image processing, in section V we present a method to detect a target using the Hough transform, in section VI we present the depth estimation using the triangulation equations and the parameters of the cameras, section VI presents the mobile robot's visual control development. Finally we arrive to the conclusion of the whole work.

II. MOBILE ROBOT MODEL

In this work is considered the unicycle mobile robot, the navigation is controlled by the speed on either side of the robot. This kind of robot has non-holonomic constraints, which should be considered during path planning. The kinematical scheme of a mobile robot can be depicted as in Fig. 1, where v is the velocity of the robot, v_l is the velocity of the left wheel, v_r is the velocity of the right wheel, r is the

radius of each wheel, l is the distance between the first two wheels, x and y are the position of the mobile robot, and ϕ is the orientation of the robot.

This type of robot can be described by the following kinematics equations:

$$\begin{cases} \dot{x} = v\cos\phi \\ \dot{y} = v\sin\phi \\ \dot{\phi} = \omega \end{cases} \quad (1)$$

The non-holonomic restriction for model (1) is

$$\dot{y}\cos\phi - \dot{x}\sin\phi = 0 \quad (2)$$

According to the motion principle of rigid body kinematics, the motion of a mobile robot can be described using equations (1) and (2), where ω_l and ω_r are the angular velocities of the left and right wheels respectively, and ω is the angular velocity.

The left and a right velocity of robot:

$$v_r = r.\omega_r \qquad v_l = r.\omega_l . \quad (3)$$

$$\omega = \frac{v_r - v_l}{l} \qquad v = \frac{v_r + v_l}{2} \quad (4)$$

Combining (2) with (3) we can obtain:

$$\omega = \frac{r}{l}(\omega_r - \omega_l) \qquad v = \frac{r}{2}(\omega_r - \omega_l) \quad (5)$$

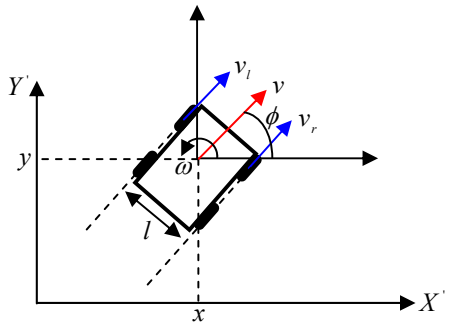

Fig. 1. Geometric description of the mobile robot

III. CAMERA MODEL

Calibration is a heavily worked on area in vision because it is necessary to estimate 3D distance information contained in an image. It allows to model mathematically the relationship between the 3D coordinates of an object in a scene and its 2D coordinates in the image [8].

The parameters of the camera are classified in two categories**, internal parameters** which define the properties of the geometrical optics and the **external parameters** which define position and orientation of the camera. More specifically, the camera calibration consists of determining the intrinsic parameters and the extrinsic parameters [9]. The model of the camera is presented in fig.2.

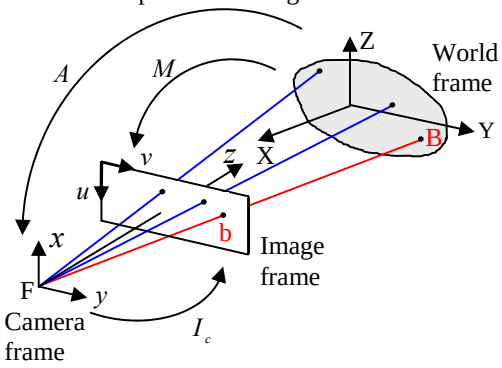

Fig. 2. Camera modele

A. Intrinsic parameters

Intrinsic parameters of the camera define the scale factors and the image centre.

$$I_c = \begin{pmatrix} \alpha_u & 0 & u_0 & 0 \\ 0 & \alpha_v & v_0 & 0 \\ 0 & 0 & 1 & 0 \end{pmatrix} \quad \begin{cases} \alpha_u = -f\ K_u \\ \alpha_v = f\ K_v \\ v_0 \\ u_0 \end{cases} \quad (6)$$

K_u, K_v represent the horizontal and vertical scale factor, f represent the focal length and u_0, v_0 represent the image centre.

B. Extrinsic parameters

Which define the transformation from the world to the camera frame given by the matrix A.

$$A = \begin{pmatrix} r_{11} & r_{12} & r_{12} & t_x \\ r_{21} & r_{22} & r_{23} & t_y \\ r_{31} & r_{32} & r_{33} & t_z \\ 0 & 0 & 0 & 1 \end{pmatrix} = \begin{pmatrix} R & T \\ 0 & 1 \end{pmatrix} \quad (7)$$

The matrix A is a combination of rotation matrix R and translation matrix T from to the world frame to the camera frame.

The transformation from the world to the image frame is given by the matrix M.

$$M = I_c\ A \quad (8)$$

We can write:

$$\begin{pmatrix} su \\ sv \\ s \end{pmatrix} = \begin{pmatrix} m_{11} & m_{12} & m_{13} & m_{14} \\ m_{21} & m_{22} & m_{23} & m_{24} \\ m_{31} & m_{32} & m_{33} & m_{34} \end{pmatrix} \begin{pmatrix} X \\ Y \\ Z \\ 1 \end{pmatrix} \quad (9)$$

In this equation X,Y,Z are the coordinates of a point B in the world frame.

IV. IMAGE PROCESSING

There exist a lot of image-processing algorithms extracting a map of the environment from the data provided by a camera But the implementation of such sophisticated algorithms is quite complex [10].

In our application the bumblebee 2 camera is used for perception. There resolution is 320x240 pixels, in this work the image processing procedure comprises four steps:

- Step1: acquisition of the two images.
- Step2: *YCbCr* image transform, when the *YCbCr* is a family of color spaces used in video systems. Y is the luminance component and *Cb* and *Cr* the chrominance components. *YCbCr* is sometimes abbreviated to YCC. *YCbCr* signals are created from the corresponding gamma adjusted *RGB* source using two defined constants *Kb* and *Kr* as follows [11]:

$$\begin{aligned} Y &= k_r \cdot R' + (1 - k_r - k_b) \cdot G' + k_b \cdot B' \\ Cb &= \frac{0.5 \cdot (B' - Y)}{(1 - k_b)} \\ C_r &= \frac{0.5 \cdot (R' - Y)}{(1 - k_r)} \end{aligned} \quad (10)$$

Where k_b and k_r are derived from the definition of the RGB space. R′, G′ and B′ are assumed to be nonlinear and to nominally range from 0 to 1, with 0 representing the minimum intensity and 1 the maximum.

Mathematical morphology is a useful tool for image segmentation and processing. Due to the complexity of color-scale morphology, we transform color image into binary image by subsampling techniques and threshold-based segmentation. Then operators in the area of binary morphology including dilation, erosion, closing and opening are used for data pre-processing [12]. Then step 3 and 4 given by follow:

Dilation operation is defined as:

$$X \oplus S = \{x / S_x \cap X \neq \Phi\} \text{ with } X = \{x / x = 1\} \quad (11)$$

Where X is the image which is to be dilated, S_x is a set of coordinate points known as structuring element

Erosion operation is defined as:

$$X \ominus S = \{x / S_x \cap X^{'} \neq \Phi\} \text{ with } X^{'} = \{x / x = 0\} \quad (12)$$

$$= \{x / S_x \cap X^{'} \neq \Phi\} \quad (13)$$

The closing operation is defined as:

$$X \bullet S = (X \oplus S) \ominus S \quad (14)$$

The closing is a dilatation followed by erosion using the same structuring element for both operations.

An opening operation is defined as

$$Y \circ S = (Y \ominus S) \oplus S \quad (15)$$

And the opening is erosion followed by dilatation

- Step3: *Cr* image plan.
- Step4: binairisation and morphology operators [12].

Right image Left image

Fig.3. images captured by the robot's stereovision system

Right image Left image

Fig.4. *RGB* to *YCbCr* color transformation

Right image Left image

Fig.5. Extraction of the *Cr* image plan

Right image Left image

Fig.6. Binarisation of the images

Right image Left image

Fig.7. Application the opening followed the closing operation

V. DETECTION THE TARGET USING HOUGH TRANSFORM

The first step correspondence algorithm is to find the circles in both images. These circles are extracted from binary edges images using the hough transform. It is a well-know method for detection of parametric curves in binary images and it was recognized as an important means of searching for objects features in binary images.

The hough transform is a robust and effective method for finding circles a set of 2D points. It is based on a transformation from the (x, y) plane (called Cartesian plane) to the (a, b, r) plane (called houghf plane). A circle is defined in the Cartesian plan by the follower equation:

$$(x-a)^2 + (y-b)^2 = r^2 \tag{16}$$

(x, y): The coordinates of the circles point in the Cartesian frame.

(r) : The radius points.

(a, b) : The coordinate of the centre circle.

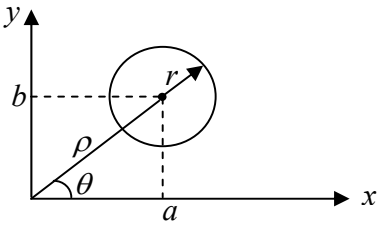

Fig.8 The circle polar parameter

The HT uses the polar parameters of the circle (Fig. 8). A circle is defined by the following equation:

$$\begin{cases} a = \rho \cos(\theta) \\ b = \rho \sin(\theta) \\ r = \sqrt{(x - \rho\cos(\theta))^2 + (y - \rho\sin(\theta))^2} \end{cases} \tag{17}$$

Where ρ is the distance between the xy plane origin and the centre circle and θ is the angle between the x axis and ρ. To detect a circle, we must determine three parameters (a, b, r), which complicate to use the hough transform in 2D. to solve this problem, we should be pass by two step, first is to find all centre circle with different radius, than is to find the radius of the circle to be detect.

We consider the hough space $H(a, b, r)$ who is in this case a space in 3D, each point of coordinate (x_i, y_i) in the xy plane corresponds the cone in the space $H(a, b, r)$ (fig. 9), and for a fixed radius it corresponds a circle in the (a, b) plan, the idea of the algorithm is to compute a and b (the coordinate of the centre circle) for each radius r, than we trace this circle in the hough space corresponding to the point of coordinate (x_i, y_i) in the xy plane. When all the circles are cut in the same point, then the good radius and the coordinate (a, b) of the point which correspond to the circle was found.

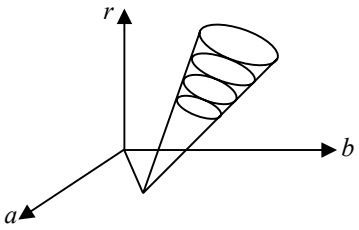

Fig.9 Hough space $H(a, b, r)$

Let θ_k be the quantification step of θ dimension and ρ_k the quantification step of ρ dimension, we compute for every discrete value of θ_i and ρ_i its corresponding points (a_j, b_j, r_j), the quantification of the plan (θ, ρ, r) returns to quantifier the interval $0 < \theta < \frac{\pi}{2}$ for the dimension of θ, and the interval $0 < \rho < \rho_{\max}$ for the dimension of ρ whit $\rho_{\max}$ is the diagonal of the image, and the interval $0 < r < r_{\max}$ for the dimension of r with $r_{\max} = \frac{\rho_{\max}}{10}$, the discrete value of θ_i, ρ_i and r_i are given by :

$$\begin{cases} \theta_i = t_1\ \theta_k & 0 < t_1 < \eta_\theta \\ \rho_i = t_2\ \rho_k & 0 < t_2 < \eta_\rho \\ r_i = t_3\ \rho_k & 0 < t_3 < \eta_r \end{cases} \tag{18}$$

With $\eta_\rho, \eta_\theta, \eta_r$ are the numbers of the discrete values in the intervals ρ, θ and r.

$$\eta_\theta = \frac{\pi}{2\ \theta_k} \quad \eta_\rho = \frac{\rho_{\max}}{\rho_k} \quad \eta_r = \frac{r_{\max}}{\rho_k} \tag{19}$$

For every point of coordinates (x, y) in the image, following the equation:

$$\begin{cases} a_j = \rho_i \cos(\theta_i) \\ b_j = \rho_i \sin(\theta_i) \\ r_j = \sqrt{(x - \rho_i \cos(\theta_i))^2 + (y - \rho_i \sin(\theta_i))^2} \end{cases} \tag{20}$$

Then, we increase by value 1, the whole cell (a_j, b_j, r_j) of the accumulator table. This cell will be increased every time an edge point lies on the circle whose the polar parameters are (a_j, b_j, r_j). Initially, all the cells values of the accumulator table are set to zero.

The choice of the (a, b, r) parameters space quantification must carry the three essential goals that are:

- good detection and precision;
- less memory storage of accumulators;
- fast implementation.

Than, we seeks the maximum of the accumulator which correspond to the circle in the edge image. By using the parameters corresponding to the maximum of the accumulator, and we compute the radius and the coordinates of the circle centre.

Right image Left image

Fig.10. Edge detection with the canny operator

Right image Left image

Fig.11. Detection the target by hough transform

Let us note, that the hough transform is robust for the parametric form detection such as the circles, the lines ……., the fig.12 and fig.13 show that in spite of degradation the edge of the target and the presence of the noises, we have got a good detection of the target.

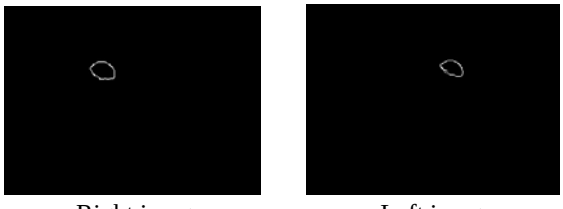

Right image Left image

Right image Left image

Fig. 12. Robustness of the hough transform in spite the degradation of the edge

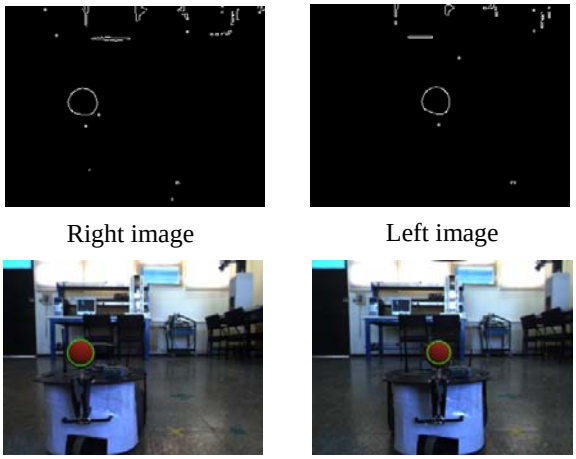

Right image Left image

Right image Left image

Fig.13. Robustness of the hough transform in the presence of noise

VI. DEPTH ESTIMATION

Depth calculates from a pair of stereoscopic images suppose the matched corresponding points between the left and right images.

If we places in the case of the three dimensional rebuilding, and if the point ${}^{l}P(x_l, y_l)$ of the left image at summer put in correspondence with the point ${}^{r}P(x_r, y_r)$ of the right image, using the equation (8) we have:

$$\begin{cases} x_l = \dfrac{m_{11}^l X + m_{12}^l\ Y + m_{13}^l\ Z + m_{14}^l}{m_{31}^l X + m_{32}^l\ Y + m_{33}^l\ Z + m_{34}^l} \\ y_l = \dfrac{m_{21}^l X + m_{22}^l\ Y + m_{23}^l\ Z + m_{24}^l}{m_{31}^l X + m_{32}^l\ Y + m_{33}^l\ Z + m_{34}^l} \\ x_r = \dfrac{m_{11}^r X + m_{12}^r\ Y + m_{13}^r\ Z + m_{14}^r}{m_{31}^r X + m_{32}^r\ Y + m_{33}^r\ Z + m_{34}^r} \\ y_r = \dfrac{m_{21}^r X + m_{22}^r\ Y + m_{23}^r\ Z + m_{24}^r}{m_{31}^r X + m_{32}^r\ Y + m_{33}^r\ Z + m_{34}^r} \end{cases} \quad (21)$$

The points ${}^{l}P$ and ${}^{r}P$ are the coordinates of the target centre calculated by hough transform.

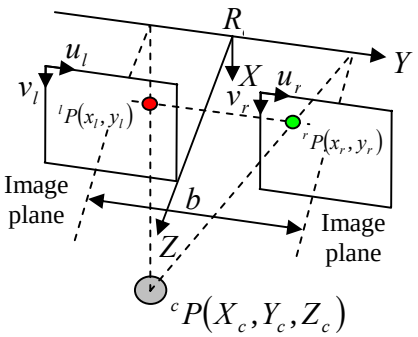

Fig.14. geometry of the stereoscopic camera

The coordinate X,Y and Z of the point P rebuilt in the calibration frame, are calculated by solving a linear system of four equations. The equation (20) can be written by:

$$\begin{pmatrix} m_{11}^l - x_l\, m_{31}^l & m_{12}^l - x_l\, m_{32}^l & m_{13}^l - x_l\, m_{33}^l \\ m_{21}^l - y_l\, m_{31}^l & m_{22}^l - y_l\, m_{32}^l & m_{23}^l - y_l\, m_{33}^l \\ m_{11}^r - x_r\, m_{31}^r & m_{12}^r - x_r\, m_{32}^r & m_{13}^r - x_r\, m_{33}^r \\ m_{21}^r - y_r\, m_{31}^r & m_{22}^r - y_r\, m_{32}^l & m_{23}^r - y_r\, m_{33}^r \end{pmatrix} \begin{pmatrix} X \\ Y \\ Z \end{pmatrix} = \begin{pmatrix} -m_{14}^l - x_l\, m_{34}^l \\ -m_{24}^l - y_l\, m_{34}^l \\ -m_{14}^r - y_r\, m_{34}^r \\ -m_{24}^r - y_r\, m_{34}^r \end{pmatrix} \quad (22)$$

The system of equation (21) can be rewritten in the form:

$$E\ P = W \quad (23)$$

We can solve the equation (22) using the least squares method:

$$P = \left(E^t\ E\right) E^t\ W \quad (24)$$

We can also rebuilt the point P in the left camera frame using the intrinsic parameters matrix of the left and right camera I_{cl}, I_{cr}. The coordinates X_g, Y_g and Z_g of the point P are given by [13]:

$$\begin{cases} Z_g = \dfrac{b}{y_1 - y_2} \\ X_g = x_1\ Z_g \\ Y_g = y_1\ Z_g \end{cases} \quad (25)$$

With: $\begin{pmatrix} x_1 \\ y_1 \\ 1 \end{pmatrix} = I_{cl}^{-1} \begin{pmatrix} x_l \\ y_l \\ 1 \end{pmatrix}$ and $\begin{pmatrix} x_2 \\ y_2 \\ 1 \end{pmatrix} = I_{cr}^{-1} \begin{pmatrix} x_r \\ y_r \\ 1 \end{pmatrix}$

By making a translation along the Y by $\dfrac{b}{2}$, the 3D coordinate of the target centre can be calculated in the frame located between the two camera left and right as is shown in fig.14. Thus the equation (25) becomes:

$$\begin{cases} Z_g = \dfrac{b}{y_1 - y_2} \\ X_g = x_1\ Z_g \\ Y_g = y_1\ Z_g - \dfrac{b}{2} \end{cases} \quad (26)$$

Thus we can calculate the distance which separates the mobile robot and the target, which are given by the following equation:

$$d = \sqrt{Y_g^{\ 2} + Z_g^{\ 2}} \quad (27)$$

The angle of deviation is given by:

$$\varphi = \tan g^{-1}\left(\frac{y_g}{Z_g}\right) \quad (28)$$

To evaluate the performances of the depth estimation using our algorithm, we took a series of measurement at different distance from the target, the results are presented by the following figures:

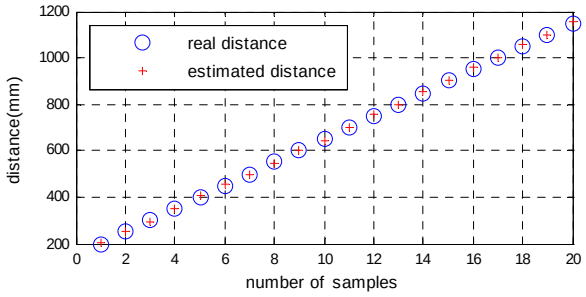

Fig.15. Variation of the real and estimated distance

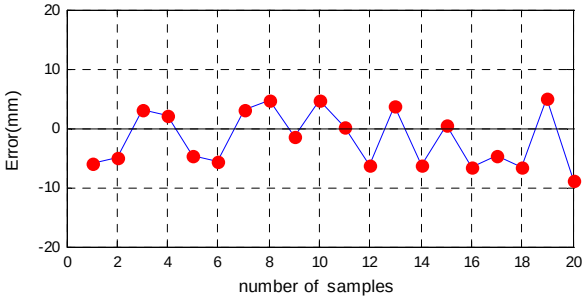

Fig.16. Error estimation of the distance

It is noticed that the error of the depth estimation varies in the interval [-10, 10 mm], which is tolerable for vision system.

VII. VISUAL CONTROL OF THE MOBILE ROBOT

In this section we describe the two different robot controllers, that have been integrated in our tracking control, the following figure illustrate the case of our application settled leader follower [17], the goal is the follower tacked the leader with conservation distance of security.

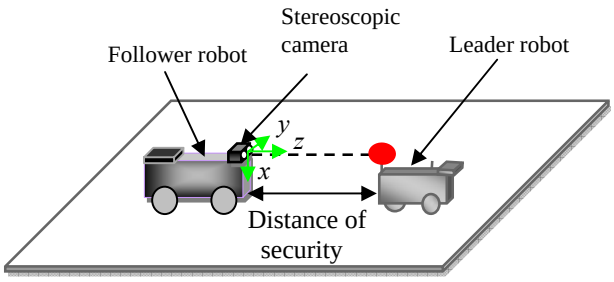

Fig.17. Configuration of our experimentation (leader-follower)

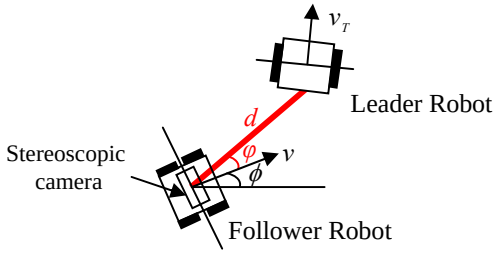

Fig.18. Relative positions between the target and the follower robot

A. Complete system design and hardware

Two Pioneer wheeled robots were used in our experiment, one as the pursuer and the other as the target. On the pursuer robot, we mounted a Bumblebee2 stereoscopic camera, which was operated at a resolution of 320×240 pixels, and it contains embedded computer with a CPU of 1.6 GHZ, the system was implemented in C++ with the openCv library of image processing [18] and the ARIA software development environment [19] running in windows XP operating system. It operated in real-time, with a calculation period of 0.3s.

a. First Controller: Non linear controller based Lyapunov method

The control objective is defined as follows: Assuming a case where a leading robot moves along an unknown trajectory, make the follower robot keep a desired distance d_d to the leader and pointing to it (that $\varphi_d = 0$), using only visual information, the control objective can be expressed as:

$$\begin{aligned} &\lim e_v(t) = \lim (d_d - d) = 0 \\ &t \to \infty \\ &\lim e_\omega(t) = \lim (\varphi_d - \varphi) = 0 \\ &t \to \infty \end{aligned} \tag{29}$$

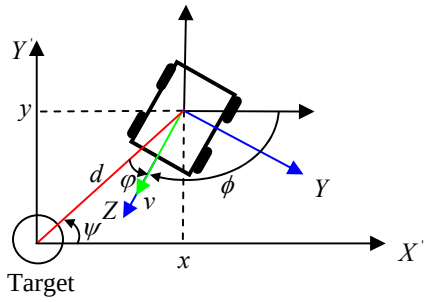

Fig.19.Representation of Variables

According to the fig.35 we have

$$\varphi = \pi + \phi - \Psi \tag{30}$$

$$d = \sqrt{x^2 + y^2} \tag{31}$$

$$\dot{d} = \frac{x\dot{x} + y\dot{y}}{\sqrt{x^2 + y^2}} \tag{32}$$

$$\begin{cases} x = d\cos(\psi) \\ y = d\sin(\psi) \end{cases} \tag{33}$$

Replacing (1) and (33) in (32) we obtain:

$$\dot{d} = -v\cos(\varphi) \tag{34}$$

$$\dot{\varphi} = \dot{\phi} - \dot{\psi} \tag{35}$$

$$\tan(\psi) = \frac{y}{x} \tag{36}$$

$$\dot{\psi} = \frac{\dot{y}x + \dot{x}y}{x^2\left(1 + \frac{y^2}{x^2}\right)} \tag{37}$$

Replacing (1) and (33) in (37) we obtain:

$$\dot{\psi} = -\frac{v}{d}\sin(\varphi) \tag{38}$$

$$\dot{\varphi} = \omega + \frac{v}{d}\sin(\varphi) \tag{39}$$

If we arrange the expression of $\dot{\varphi}$ and $\dot{d}$ into matrix form we get:

$$\begin{bmatrix} \dot{d} \\ \dot{\varphi} \end{bmatrix} = \begin{bmatrix} -\cos(\varphi) & 0 \\ \frac{1}{d}\sin(\varphi) & 1 \end{bmatrix} \begin{bmatrix} v \\ \omega \end{bmatrix} \tag{40}$$

The evolution of the posture of the follower robot relative to the leader will be stated by the time derivative of the two error variables, the variation of distance is given by:

$$\dot{e}_v = \dot{d}_d - \dot{d} = -\dot{d} \tag{41}$$

$$\dot{e}_v = v\cos(\varphi) \tag{42}$$

Likewise the variation of the angle error is given by:

$$\dot{e}_\omega = \dot{\varphi}_d - \dot{\varphi} = -\dot{\varphi} \tag{43}$$

$$\dot{e}_\omega = -\left(\omega + \frac{v}{d}\sin(\varphi)\right) \tag{44}$$

Posing:

$$\begin{cases} \dot{e}_v = -f_{e_v}(e_v) \\ \dot{e}_\omega = -f_{e_\omega}(e_\omega) \end{cases} \tag{45}$$

The non linear controller is calculated by:

$$\begin{cases} v = \dfrac{-1}{\cos(\varphi)} f_{e_v}(e_v) \\ \omega = f_{e_\omega}(e_\omega) - \dfrac{v}{d}\sin(\varphi) \end{cases} \quad (46)$$

$f_{e_v}(e_v)$, $f_{e_\omega}(e_\omega) \in \Gamma$ with Γ the set function that meet the following definition:

$$\Gamma = \{f : \Re \to \Re \,/\, f(0) = 0 \; and \; x\, f(x) > 0 \;\forall\; x \in \Re\}$$

We chose the function $f_{e_v}(e_v)$, $f_{e_\omega}(e_\omega)$ used in [20]:

$$\begin{cases} f_{e_v}(e_v) = k_{e_v} \tanh(\lambda_{e_v} e_v) \\ f_{e_\omega}(e_\omega) = k_{e_\omega} \tanh(\lambda_{e_\omega} e_\omega) \end{cases} \quad (47)$$

With : k_{e_v} , λ_{e_v} , k_{e_ω} , λ_{e_ω} is positive gain.

The variable by this controller (φ, d) as given by the equation (27) and (28) are calculated by the stereovision system.

• Stability analysis

Let us consider Lyapunov function as follows:

$$V = \frac{1}{2}\left(e_v^2 + e_\omega^2\right) > 0 \quad (48)$$

The derivative of (48) is given by:

$$\dot{V} = e_v\, \dot{e}_v + e_\omega\, \dot{e}_\omega \quad (49)$$

$$\dot{V} = -e_v\, f_{e_v}(e_v) - e_\omega\, f_{e_\omega}(e_\omega) < 0 \quad (50)$$

It than concluded the asymptotic stability is verified.

We generate a circular and sinusoidal trajectory at the leader mobile robot, the parameters of the leader robot (angular and linear velocity) and the controller is shown in the following table.

Table.3 Parameters the leader robot and the controller

	Parameters	Quantity
leader	$v_T(t)$ $[mm/s]$	200
	$\omega_T(t)$ [deg/ s]	8
	d_d $[mm]$	500
controller	k_{e_v}	360
	λ_{e_v}	0,005
	k_{e_ω}	10
	λ_{e_ω}	0,1

To illustrate the efficiency of the proposed non linear controller, the experimental results is shown in the follower figures, in fig.20 and fig.24 we not that the relative distance between the leader and the follower robot is maintained constant with the desired distance, the fig.21 and fig.25 show the evolution of angle φ , the fig.22 and fig.26 show the control actions are calculated and sent to the follower robot, and the trajectory carried by the two robots is shown in fig.23 and fig.27.

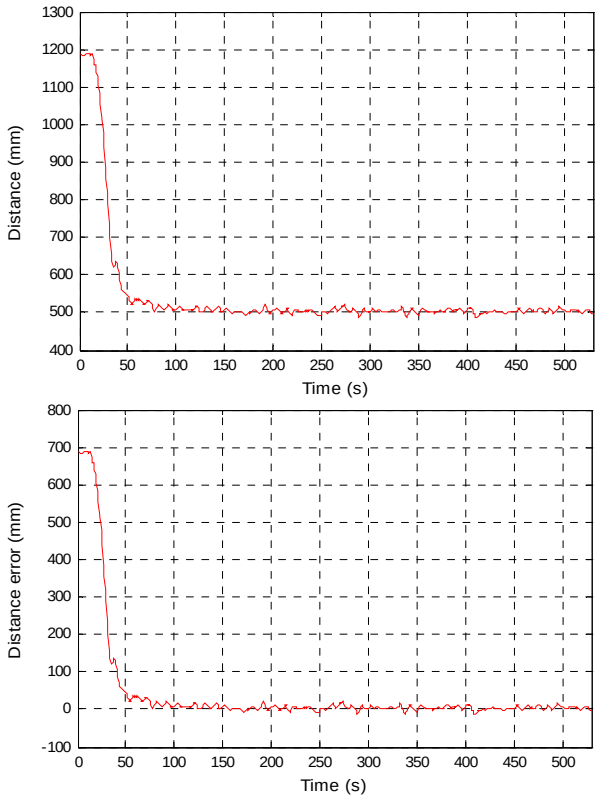

Fig.20. Evolution of the distance and error

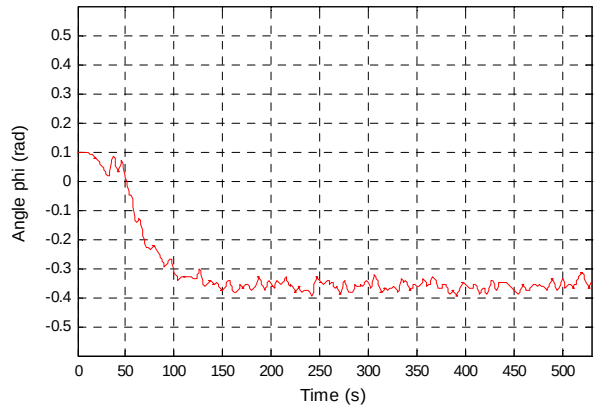

Fig.21. Evolution of the angle φ

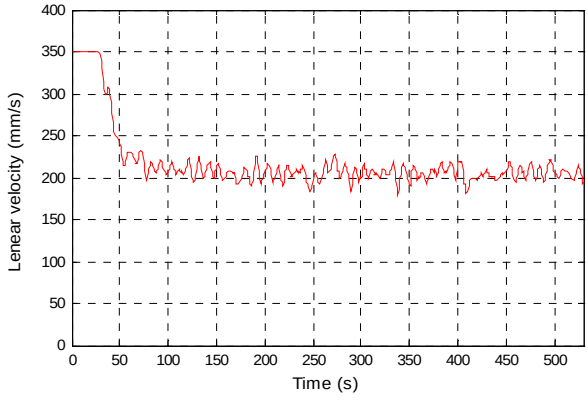

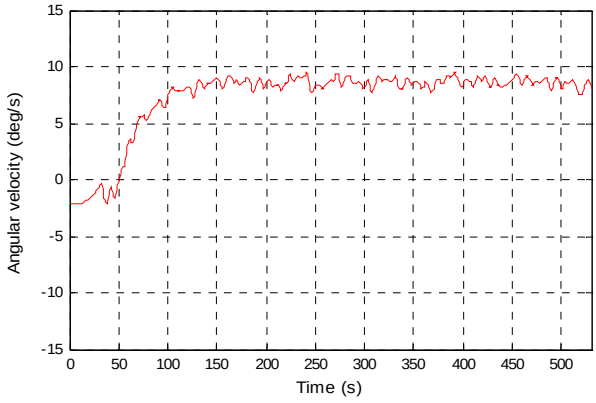

Fig.22. Desired control action

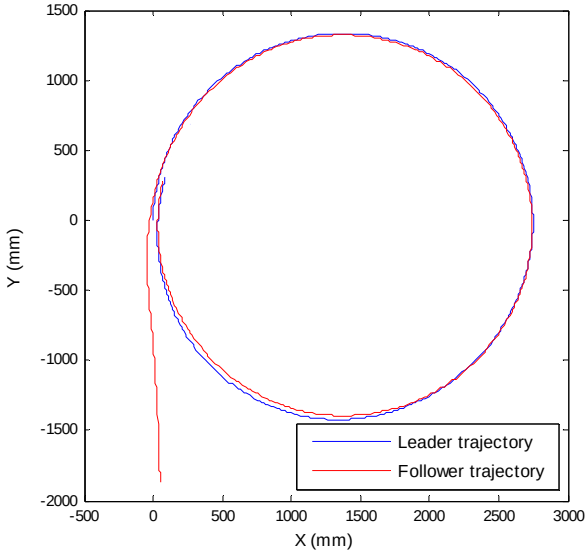

Fig.23. Trajectories followed by the leader and the follower robots

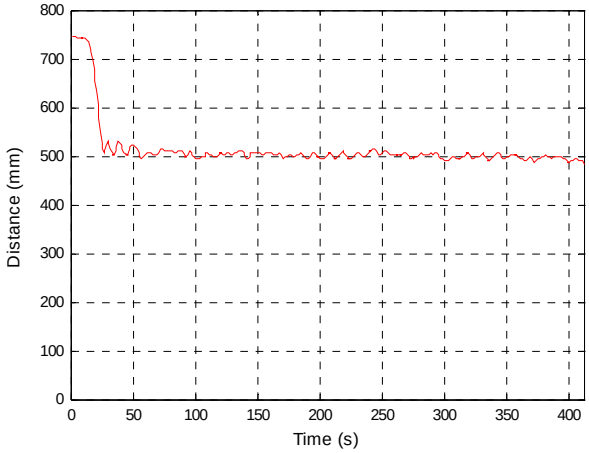

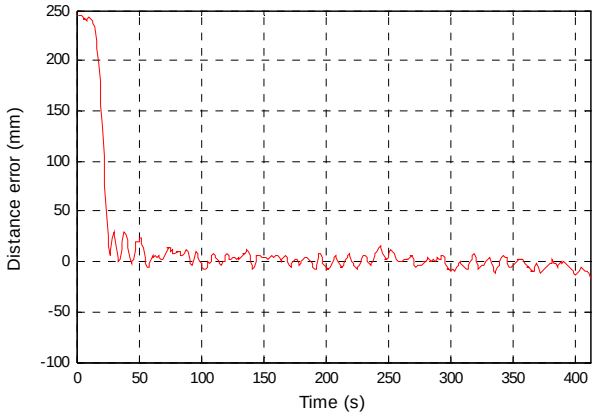

Fig.24. Evolution of the distance and error

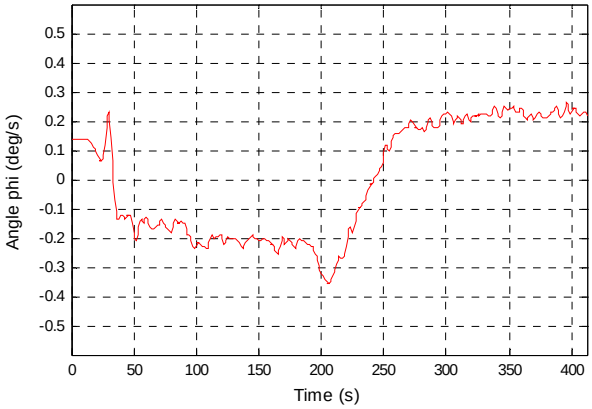

Fig.25. Evolution of the angle φ

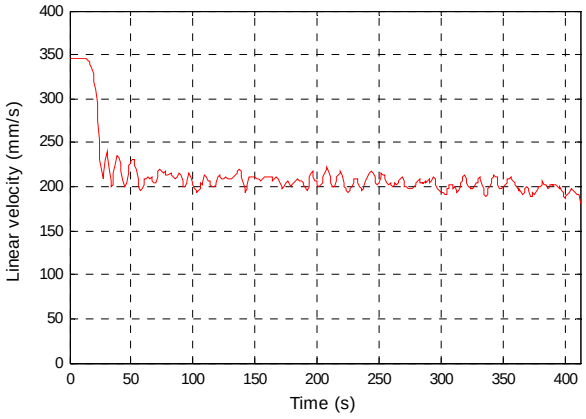

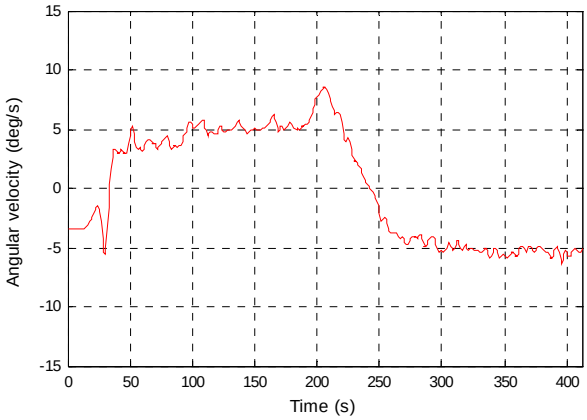

Fig.26. Desired control action

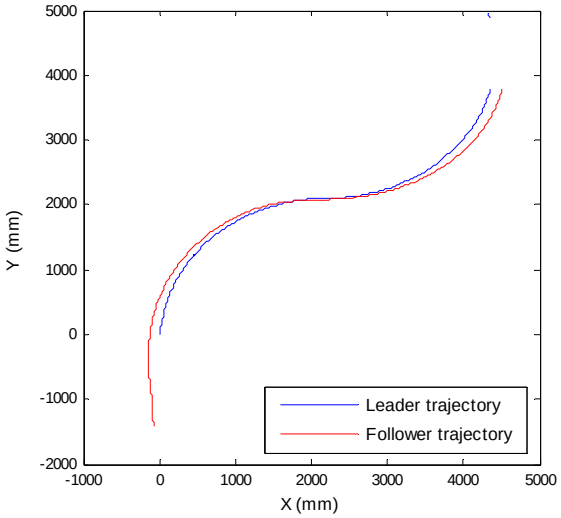

Fig.27. Trajectories followed by the leader and the follower robots

b. Second Controller: Fuzzy logic controller

The fuzzy logic is presented by the philosopher Maxblock since 1937, the concept of fuzzy logic was really introduced in 1965 by L.zadeh [21]. It is based on the mathematical theory of the fuzzy subsets, the aptitude of fuzzy logic reside in the handling of the imprecise measurements used by the human language. The number of application based on this logic increased in last years considerably, this is due to the fact that fuzzy logic is usually expressed by linguistic rules (if-than). However, this theory is still too recent to achieve the unanimity within the scientific community.

In this section, the vision based tracking control of the follower mobile robot using the proposed fuzzy logic controller is presented. For translation velocity and angular velocity controls, tow controllers FLC1 and FLC2 are adopted, respectively. Let the input variables of the FLC1 and FLC2 be defined as:

$$e_{fv} = d - d_d \tag{51}$$

$$e_{f\omega}(k) = \varphi_d - \varphi \tag{52}$$

We want to design the two fuzzy logic controllers FLC1 and FLC2 for the follower mobile robot such that it can pursue the target mobile robot within a constant distance. The fuzzy control rules can be represented as a mapping from input linguistic variables $e_{fv}(k)$, $\Delta e_{fv}(k)$ to output linguistic variables v and ω as follows:

$$v = \text{FLC1}\left(e_{fv}\right) \tag{53}$$

$$\omega = \text{FLC2}\left(e_{fv}\right) \tag{54}$$

The membership functions of input linguistic variables $e_{fv}(k)$, $e_{f\omega}(k)$ and the membership functions of output linguistic variables v and ω are shown in fig.28.

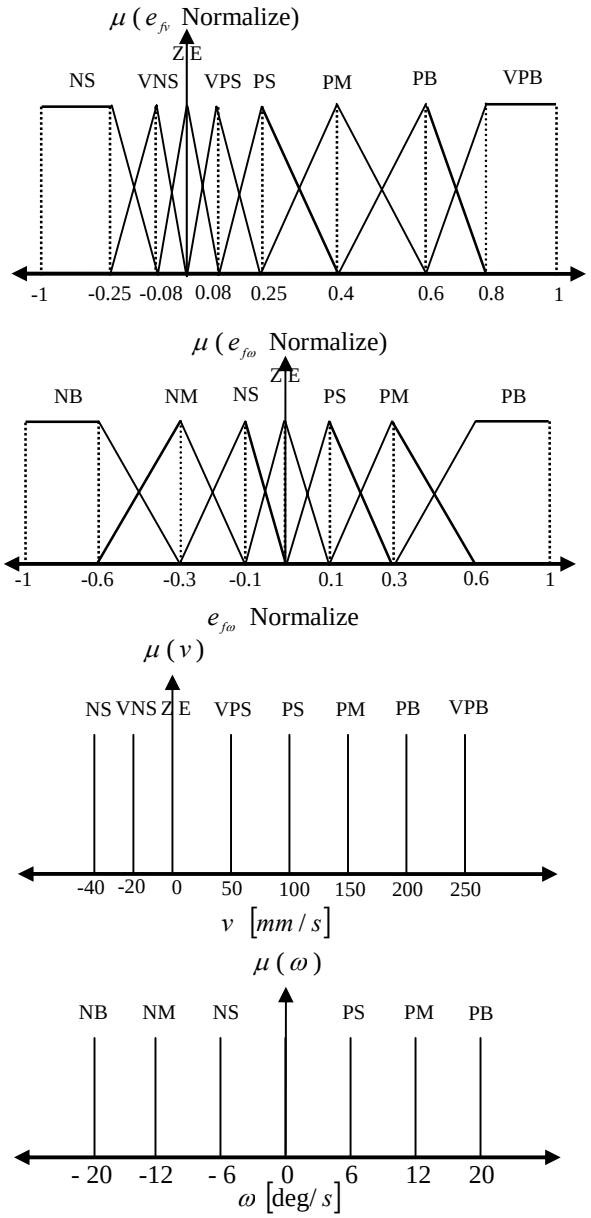

Fig.28. Membership function of the inputs $(e_{fv}, e_{f\omega})$ and output (v, ω)

Table.1 Rule table of the FLC1 and FLC2

FLC1	e_{fv}	NS	VNS	ZE	VPS	PS	PM	PB	VPB
	v	NS	VNS	ZE	VPS	PS	PM	PB	VPB
FLC2	$e_{f\omega}$	NB	NM	NS	ZE	PS	PM	PB	-
	ω	NB	NM	NS	ZE	PS	PM	PB	-

The input of the FLC1 (e_{fv}) is decomposed into eight fuzzy partitions, such as: negative small (**NS**), very negative small (**VNS**), zero (**ZE**), very positive small (**VPS**), positive small (**PS**), positive medium (**PM**), positive big (**PB**) and very positive big (**VPB**). The input of the FLC2 $(e_{f\omega})$ is decomposed into seven fuzzy partitions, such as: negative big (**NB**), negative medium (**NM**), negative small (**NS**), zero (**ZE**), positive small (**PS**), positive medium (**PM**), and positive big (**PB**).

The input (e_{fv}) is divided into eight fuzzy sets and $(e_{f\omega})$ is divided into seven fuzzy sets, 8 fuzzy rules for linear velocity control and 7 fuzzy rules for angular velocity control. The defuzzification strategy is implemented by the weighted average method.

$$u = \frac{\sum_{j=1}^{N} \mu_j(u_j) u_j}{\sum_{j=1}^{N} \mu_j(u_j)} \tag{55}$$

N is the number of the rules.

Where μ may be the linear velocity or angular velocity command of the tracker mobile robot, u_j is the support of each fuzzy set j, and u is the membership function value of each rule.

We generate circular and sinusoidal trajectories for the leader mobile robot, the parameters of the leader robot (angular and linear velocity) are shown in the following table.

Table.1 Parameters the leader and the controller

	Circular trajectory	Sinusoidal trajectory
$v_T(t)$ $[mm/s]$	200	200
$\omega_T(t)$ [deg/ s]	8	$\begin{cases} +5 & 0 < t < 200\ s \\ -5 & 200\ s < t < 412\ s \end{cases}$
d_d $[mm]$	500	500

The experimental results are presented in the following figures, in fig.29 and fig.33 we not that the fuzzy controller given a satisfied performance and a good tracking by the follower robot by maintaining the desired distance without static error, the fig.30 and fig.34 show the evolution of angle φ , the fig.31 and fig.35 show the control actions are calculated and sent to the follower robot , finally the trajectory of the leader and follower robot is depicted in fig.32 and fig.36.

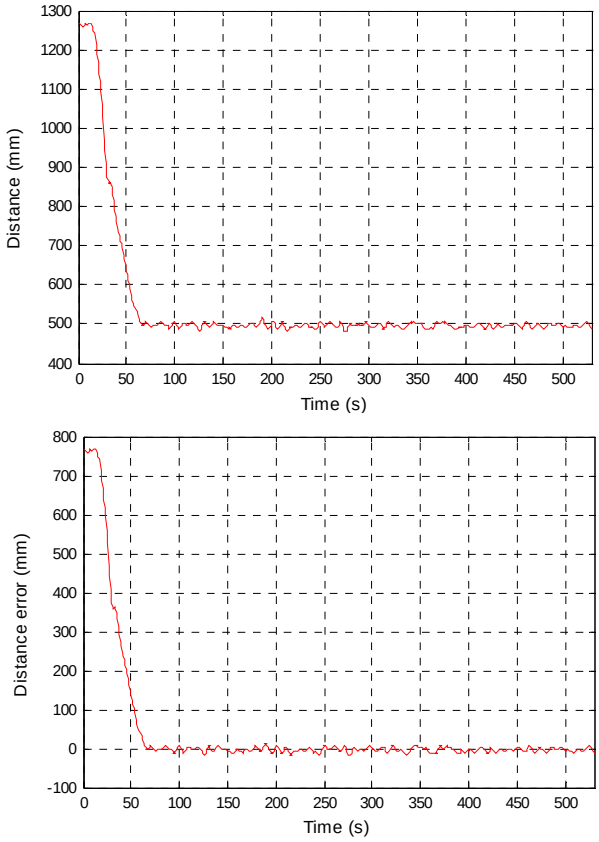

Fig.29. Evolution of the distance and error

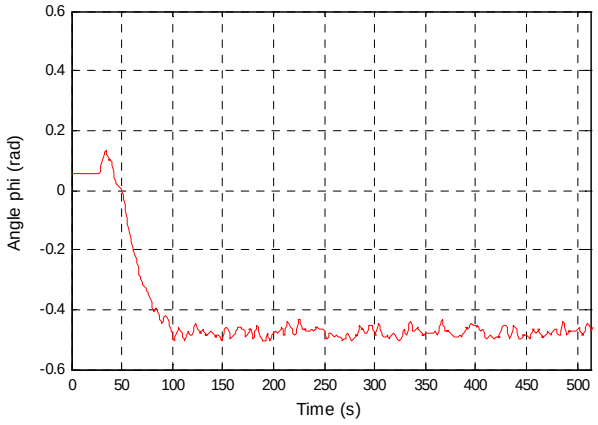

Fig.30. Evolution of the angle φ

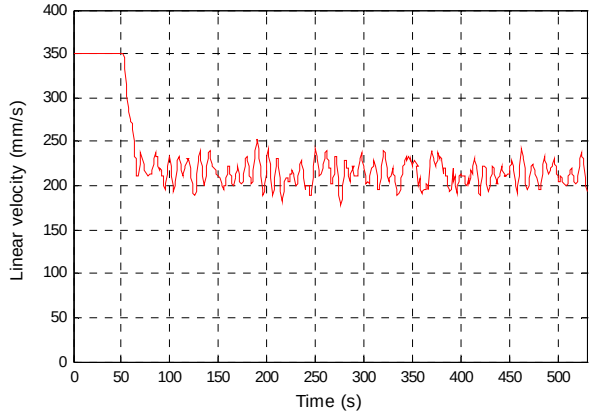

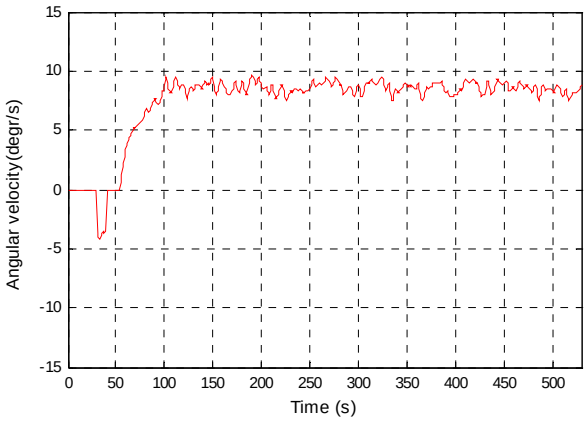

Fig.31. Desired control action

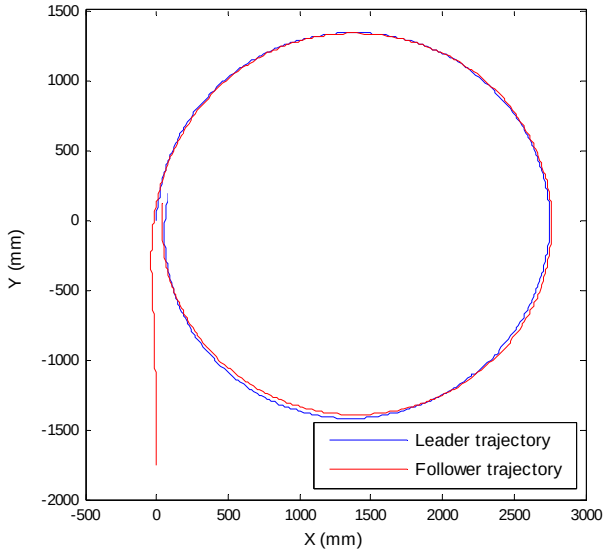

Fig.32: Trajectories followed by the leader and the follower robots

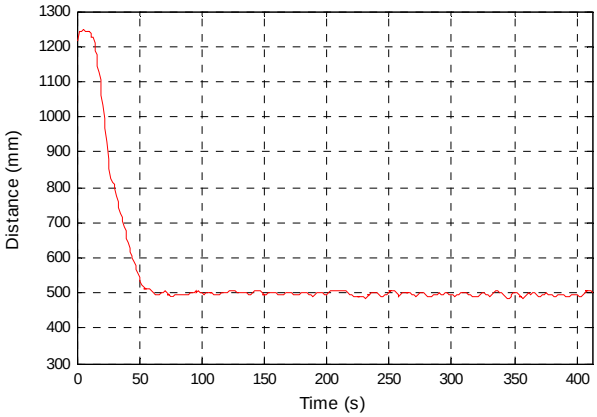

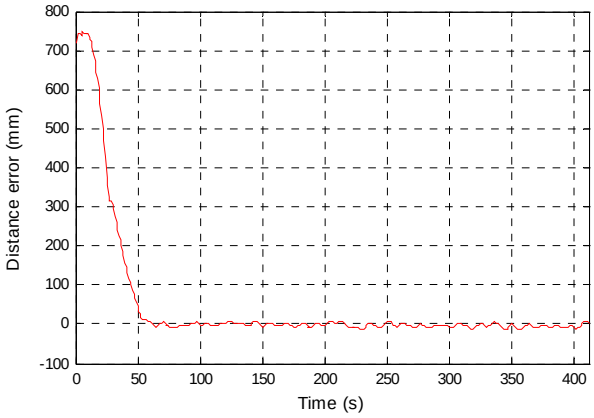

Fig.33. Evolution of the distance and error

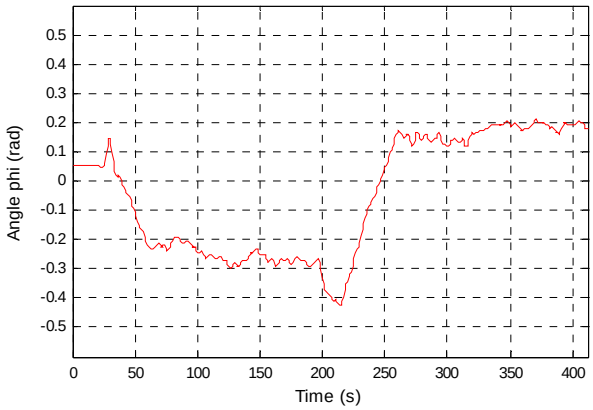

Fig.34. Evolution of the angle φ

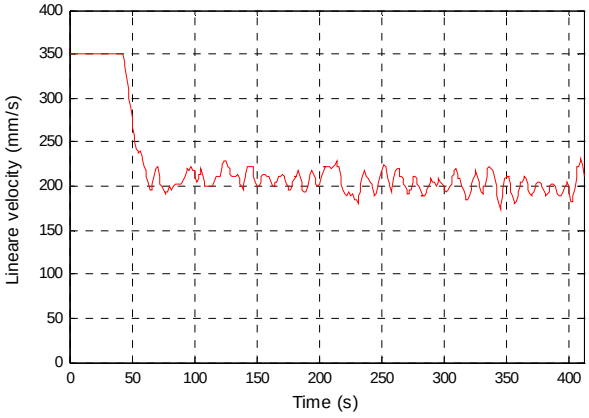

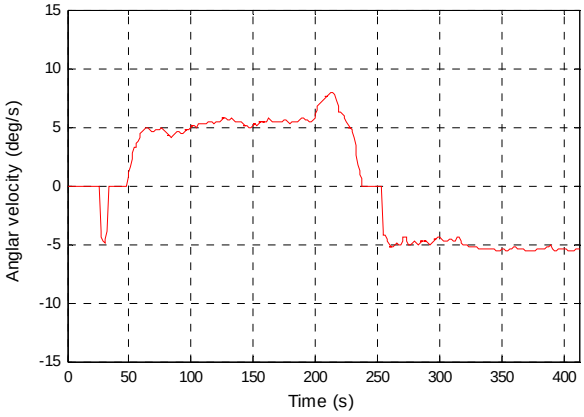

Fig.35. Desired control action

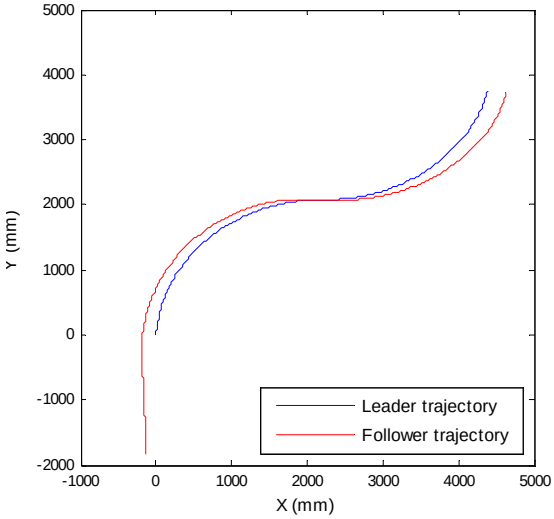

Fig.36. Trajectories followed by the leader and the follower robots

VIII. CONCLUSION

This paper proposes two vision-based tracking control approaches for nonholonomic robot, for objective is the tracker robot follows a target vehicle by maintaining a desired distance. In spite of its implementation simplicity, but it seems clearly the Lyapunov controller is more preferment than the fuzzy logic controller specially on terms of tracking accuracy. Finally, we can say that the different experimental results verified availability of our proposed approaches.

REFERENCES

[1] D. Burschka, J. Geiman, and G. Hager, "Optimal landmark configuration for vision-based control of mobile robot," Proceedings of the 2003 IEEE International Conference on Rob. and Auto. , Taipei, Taiwan, 2003.

[2] N. J. Cowan, D. E. Koditschek, "Planar image based visual servoing as a navigation problem," Proceedings of the 1999 IEEE International Conference. *Conf. on Rob. and Auto.,*Detroit, Michigan, 1999.

[3] G. N. DeSouza, A. C. Kak, "Vision for Mobile Robot Navigation: A Survey," IEEE TRANSACTIONS ON PATTERN ANALYSIS AND MACHINE INTELLIGENCE, VOL. 24, NO. 2, FEBRUARY 2002.

[4] L. Freda, G.Oriolo, "Vision based interception of a moving target with a nonholonomic mobile robot," Science direct on Robotics and Autonomous Systems 55 (2007) 419– 432.

[5] C. Tsai, K.Song, "Robust visual tracking control of mobile Robot Based an error model in Image Plane," Proceedings of the 2005 IEEE International Conference on Mechatronics & Autoation, July, April 2005.

[6] R. Choomuang, N. Afzulpurkar, "Hybrid Kalma Filter/Fuzzy Logic based Position Control of Autonomous Mobile Robot," *International Journal of Advanced Robotic Systems, Volume 2, Number 3 (2005), ISSN 1729-8806.*

[7] H. Kannan, V.Chitrakaran, D. M. Dawson and T. Burg ,"Vision-based Leader/Follower tracking for Nonholonomic mobile robots," Proceedings of the 2007 American control conference, New York City, USA, July 11-13, 2007.

[8] T. S. Li, S.J Chang, and Wei Tong, "Fuzzy Target Tracking Control of Autonomous Mobile Robots by Using Infrared Sensors," IEEE TRANSACTIONS ON FUZZY SYSTEMS, VOL. 12, NO. 4, AUGUST 2004.

[9] M. Sisto, "A Fuzzy Leader-Follower Approach to Formation Control of Multiple Mobile Robots," Proceedings of the 2006 IEEE/RSJ International Conference on Intelligent Robots and Systems, October 9 - 15, 2006, Beijing, China.

[10] E. Trucco., A. Verri, "Introductory techniques for 3-D computer vision," chapter 6, Prentice Hall, 1998.

[11] G.Toscani, "Système de Calibration et perception du mouvement en vision artificielle," Ph.D. Thesis -Université Paris Sud – 15 dec. 1987.

[12] R. K Lenz, R. Y. Tsai, "Technique for calibration of scale factor and image center for high accuracy 3D machine vision metrologie,". IEEE Transactions on Pattern Analysis and Machine Intelligence – 1988.

[13] J-B. Coulaud, G. Campion, G. Bastin, and M. De Wan ,"Stability Analysis of a Vision-Based Control Design for an Autonomous Mobile Robot," IEEE TRANSACTIONS ON ROBOTICS, VOL. 22, NO. 5, OCTOBER 2006.

[14] R. Montúfar-Chaveznava, F. H. Gallardo and S. P.Hernández, "Face Detection by Polling," 2005 IEEE, Portugal, pp 292-297, September 2005.

[15] Z. Hai-bo, Y. Kui, L. Jin-dong "A Fast and Robust Vision System for Autonomous Mobile Robots," Proceedings of the 2003 IEEE International Conference on Robotics, Intelligent systems and signal processing, October, 2003, Changsha, China.

[16] R Horaud, O. Monga, "*Vision Par Ordinateur*," Edition Hermès, deuxieme Edition, France 1995.

[17] A.K. Das, R. Fierro, V. Kumar, J.P. Ostrowsky, J.Spletzer, and C. Taylor, "A vision-based formation control framework," *IEEE Trasaction on Robotics and Automation*, VOL. 18, NO. 5, OCTOBER 2002.

[18] User guide of the OpenCv library http://opencvlibrary.sourceforgr.net.

[19] Active media.

[20] R. Carelli, C. M.Soria and B.Morales," Vision-Based Traking Control for mobile Robot,", International conference on robotic & Autmation, Argentina, July 2005.

[21] K. M. Passino "Fuzzy control," Departement of Electrical Engineering the ohio sate university 1998.